LBL-24486
Preprint

Lawrence Berkeley Laboratory
UNIVERSITY OF CALIFORNIA

RECEIVED
LAWRENCE
BERKELEY LABORATORY

APR 19 1988

LIBRARY AND
DOCUMENTS SECTION

Submitted to Physical Review C

The Apparent Violation of Isospin Symmetry in the $^3H(^3He,^2H)^4He$ Reaction

G. Rai, C.O. Blyth, J.B.A. England, A. Farooq,
O. Karban, E. Rawas, S. Roman, and R. Vlastou

December 1987

TWO-WEEK LOAN COPY

This is a Library Circulating Copy which may be borrowed for two weeks.

NUCLEAR SCIENCE DIVISION

LBL-24486 c.2

Prepared for the U.S. Department of Energy under Contract DE-AC03-76SF00098

DISCLAIMER

This document was prepared as an account of work sponsored by the United States Government. While this document is believed to contain correct information, neither the United States Government nor any agency thereof, nor the Regents of the University of California, nor any of their employees, makes any warranty, express or implied, or assumes any legal responsibility for the accuracy, completeness, or usefulness of any information, apparatus, product, or process disclosed, or represents that its use would not infringe privately owned rights. Reference herein to any specific commercial product, process, or service by its trade name, trademark, manufacturer, or otherwise, does not necessarily constitute or imply its endorsement, recommendation, or favoring by the United States Government or any agency thereof, or the Regents of the University of California. The views and opinions of authors expressed herein do not necessarily state or reflect those of the United States Government or any agency thereof or the Regents of the University of California.

The Apparent Violation of Isospin Symmetry in the $^3H(^3He,^2H)^4He$ Reaction*

G. Rai[1], C. O. Blyth[2], J. B. A. England[2], A. Farooq[3], O. Karban[2], E. Rawas[4], S. Roman[2], R. Vlastou[5]

[1]Lawrence Berkeley Laboratory, University of California
MS70A-3307, Berkeley, CA 94720, USA

[2]Department of Physics, University of Birmingham
P. O. Box 363, Birmingham B15 2TT, UK

[3]Royal Signals and Radar Establishment, Malvern, WORCS., U.K

[4]Department of Physics, University of Mecca
P.O. Box 6675, Mecca, Saudi Arabia

[5]Department of Physics National Technical University
of Athens, Athens, Greece

Abstract:

Angular distributions of the vector analyzing powers for the $^3H(^3He,^2H)^4He$ reaction have been measured over the incident energy range 18-33 MeV. The measurements centered about 18 MeV display a deviation from the antisymmetric shape expected from isospin symmetry. Concentrating on the explanation of the 90° analyzing powers, we report the results of a DWBA analysis which includes the direct and exchange processes and the spin-orbit potential. It is shown that the anomalous behavior of the 90° vector analyzing powers can be largely explained by the effect of a single F-wave potential resonance which leads to the magnification of the short-range differences between the ^3He and ^3H wave functions.

1. INTRODUCTION

It is generally believed that isospin is conserved in fast reactions between light nuclei, and therefore considerable effort has been made in the past to understand why pronounced deviations from symmetry about 90° cm occur in the $^{4}He(^{2}H,^{3}He)^{3}H$ reaction cross sections. Prior to present investigation, vector analyzing powers and cross sections had been measured at only a few energies in the 10-35 MeV range[1-2]. For the reaction $^{3}He(^{3}H,^{2}H)^{4}He$, analyzing power measurements had been reported by Haglund et al.[3]. These were limited to incident triton energies below 18 Mev and exhibited the most striking and unexpected behaviour, i.e., raising the beam energy is accompanied by a consistently increasing negative analyzing power at 90° (c.m) scattering angle.

Unlike the situation for the $^{4}He(^{2}H,^{3}He)^{3}H$ reaction, where the assumption of isospin conservation leads in a model-independent way to the antisymmetry of the deuteron analyzing power (the so-called Barshay-Temmer (B-T) theorem (see ref. 4)), several restrictions on the allowed direct processes are required before antisymmetry of the $^{3}He(^{3}H,^{2}H)^{4}He$ analyzing power is predicted. However, the cross section should always be symmetric for a direct reaction provided (a) the nuclei in either the entrance or exit channel are exact isospin partners, (b) channel isospin is conserved and is unique. In their paper, Haglund et al.[3] introduce the general formalism to describe the $^{3}He(^{3}H,^{2}H)^{4}He$ reaction and re-derive the more specialized predictions of Conzett[5]. The Conzett model of the reaction includes only the direct and exchange amplitudes for single particle transfer. As a result, the antisymmetry of the vector analyzing power about

90° (θ_{cm}) is predicted assuming the nucleon-nucleon force is charge symmetric. In the subsequent discussion we accept this result as a naive generalization of the B-T theorem which might suitably describe the $^{3}He+^{3}H \leftrightarrow d+\alpha$ reaction at high energies.

The analyzing power angular distributions for the $^{3}He(^{3}H,^{2}H)^{4}He$ reaction at bombarding energies of 9.02, 12.3 and 17.0 MeV (and the corresponding excitation function at 90° cm) are shown in ref. 3. The most noticeable features of the data are the pronounced, energy-dependent deviations from antisymmetry, which are much larger in magnitude (fore-aft asymmetries of up to 40%) than those found by Dahme et al.[2] in the $^{4}He(d,^{3}H)^{3}He$ reaction at E_{d} = 32 MeV (22.8 MeV excitation in ^{6}Li). As Haglund et al. point out, this difference is not necessarily surprising since the combination of scattering matrix elements which appear in the expression for the $^{3}H(^{3}He,d)^{4}He$ vector analyzing power is entirely different from that which appears in the formula used to calculate the $^{4}He(d,^{3}H)^{3}He$ values. Nevertheless, it is remarkable to observe such gross deviations from antisymmetry.

In general terms, the literature on the subject admits three plausible explanations, which are briefly recapitulated here. First, the deviations may be due initially to the distortion of the deuteron in the Coulomb field of the ^{4}He nucleus, but a rough estimate of the possible T=1 admixture, made by Drachman[6], appears to preclude this possibility at these high energies. Secondly, Nocken et al.[7] concluded that, while the main part of the $^{3}H(^{3}He,d)^{4}He$ reaction at low energy, $E(^{3}He)$ = 800 keV, proceeds via a

$(J^{\pi},T)=(1^{-},0)$ resonance in ^{6}Li, the asymmetry of the cross section angular distribution arises from the interference between that resonance and a simultaneously excited, isospin-forbidden $(J^{\pi},T)=(2^{+},1)$ resonance. That is, at higher energies a reaction mechanism more complicated than the one underlying the Conzett model may be needed to explain the observed deviations from antisymmetry in the analyzing power data. Thirdly, deviations from symmetry in the $^{4}He(d,^{3}He)^{3}H$ cross-section data of Gross et al.[1] have been explained by Richter and Vincent[8] and Werby and Robson[9] in terms of slightly different neutron and proton transfer amplitudes.

A detailed examination of the direct reaction mechanism has been carried out by Edwards et al.[10] using the DWBA theory. They calculated all possible combinations of direct or exchange, nucleon or core, transfers and demonstrated that the knock-out interaction potential is mainly diagonal and its matrix elements cancel with those of the optical potential. Thus the "usual DWBA cancellation assumption" is justified for these light ion reactions--a result confirmed by their prediction of the $^{4}He(d,^{3}He)^{3}H$ cross section at an incident energy equivalent to 26 MeV ^{3}He.
Hence we conclude that, particularly near 90°, the DWBA treatment of the Conzett model should give accurate predictions. The failure of the model at some energies is therefore a clear indication of either the inadequacy of the model (for example, because of the involvement of mixed isospin intermediate states) or the nonconservation of charge symmetry in nuclear forces.

Before deciding on the formation of isospin-forbidden resonances in the compound ^{6}Li system, a comprehensive DWBA analysis of the cross-section data, and particularly the analyzing-power data, is required. Our treatment

of this reaction differs from earlier investigations in that most DWBA calculations have neglected the polarization observables or ignored the Coulomb effects or the spin-orbit potential. More importantly, there was an urgent need to extend the vector analyzing power measurements for the $^{3}H(^{3}He,^{2}H)^{4}He$ reaction to higher energies in order to gain an insight into the trends noted by Haglund et al. In addition, it was desirable to study this reaction at an energy high enough to ensure the dominance of the direct mechanism.

In the following section the new experimental data are presented. Section 3 outlines a DWBA model of the reaction, and in sections 4 and 5 the salient points arising from an investigation of the data at 18 and 33 MeV are discussed.

II. THE EXPERIMENT AND RESULTS

A 33.2 MeV polarized ^{3}He beam was provided by the University of Birmingham Radial Ridge cyclotron and scattered from a tritium target. The beam energy was degraded as necessary with the aid of aluminium foils and a series of analyzing power angular distributions at 18, 20, 24, 27 and 33 MeV incident energies (24-32 MeV excitation in ^{6}Li) were obtained.[11].

A. The Target

The natural choice of a target for this experiment is tritium gas. However, to avoid handling the radioactive gas, a solid target[12] was used for this experiment. The target consisted of 0.8 mg cm^{-2} tritiated titanium film bonded to a 39.5 mg cm^{-2} copper backing for stability and to increase heat conduction away from the beam spot. The tritium content was about 0.048 mg cm^{-2}.

Although this target was much safer to handle, the copper-titanium backing led to substantial background. This created the difficulty of having to separate out the large numbers of similar particles from other reactions and indeed required the use of special methods when identifying the genuine deuterons from the $^{3}H(^{3}He,d)^{4}He$ two-body reaction at large scattering angles. The use of this target also led to another uncertainty about the final results. To obtain data at some angles the target was set at an angle or even reversed for data taking at the very large angles. The uncertainty about the exact target shape led to uncertainty as to whether the changes in energy loss were correctly compensated for in each case. It is estimated that systematic variations of up to 0.5 MeV from the listed mid-target energy could have occurred at some angles.

B. The Counter Telescope Measurements

(a) The forward angle measurements were made using conventional particle telescope counters. The technique is widely known and will not be described here in detail. Briefly, the incoming polarized ^{3}He beam struck the tritium target located at the center of a scattering chamber. Three counter telescopes, each containing two silicon detectors in the usual ΔE (100 μm), E'(5 mm Li drifted) arrangement, were mounted on each of the left and the right arms in the chamber.

The counter telescopes were set at equal angles left and right of the incident beam direction. With the beam spin polarization in the up direction (i.e., perpendicular to the reaction plane), the deuteron energy spectra in the left and right telescopes were recorded for a preset amount of integrated

beam charge. The spin polarization was then reversed and data taken for the same amount of integrated charge. This switching procedure was repeated many hundreds of times before the results were totalled for each spin state.

The observed energy spectrum, shown in figure 2 is dominated by background deuterons originating from two body and breakup reactions on the copper/titanium backing. Fortunately, the large positive Q value (14.32 MeV) of the $^{3}H(^{3}He,^{2}H)^{4}He$ reaction ensured that the forward-going deuterons ($\leq 40^{o}$ lab) were separated from the background. For angles above 40° the deuteron peak merged with the background and was usually indistinguishable for incident energies other than 33 MeV. A more complicated technique was required to complete the angular distributions in regions where the yield of two-body deuterons is low because of the relatively small cross section and beam current.

(b) In the second part of this experiment, the forward-scattered deuterons were detected in coincidence with the associated (recoil) alpha particles. The experimental set-up is shown schematically in Figure 1. Three counter telescopes, positioned 5° apart as before, were mounted 300 mm from the target on the left arm. Coincidences were sought between signals from any one of the telescopes and those from the large area, surface barrier, detector (L.A.D) located on the right arm behind a 26mm-wide by 10mm-high rectangular aperture. The L.A.D. was positioned 100 mm from the target center and subtended an angle of 16° at the target center. Because the geometrical requirements for coincident detection are a function of scattering angle and incident beam energy, they could not always be satisfied in practice, given the finite size of the large area detector. Under these circumstances,

coincidences were sought between the large area detector and only two of the counter telescopes. At angles about 90° cm the energetic deuterons were detected in the counter telescopes while the recoil alphas were stopped in the large area detector. Some backward angle measurements (greater than 120°) were made by detecting the forward-going alpha particles in the counter telescopes, while the recoil deuterons were detected in the L.A.D. If a coincidence occurred, the energy signals from the appropriate ΔE-E' counter telescope were summed with the energy signal from the L.A.D. Consequently, the large Q-value of this reaction separated the total energy (true coincidence) peak from the predominantly low-energy background. This aided the extraction of the wanted data.

The signals from the ΔE-E' configured telescopes were processed in the same way as before. However, a fast timing signal derived from the ΔE1 passing detector, was used to stop a time-to-amplitude converter TAC, whose conversion cycle was initiated by a "start" pulse derived from the L.A.D. Thus, the output signal from the TAC represented the difference in flight time between a deuteron detected in the counter telescope and a (recoil alpha) particle arriving at the L.A.D.

The mass signal from the ΔE-E telescope particle identifier was adjusted to reject all but the deuteron mass recognition pulses and provided a logic input to a slow coincidence unit. Two other slow coincidence inputs were derived from outputs belonging to the (E') stopping detector and the TAC unit. The output from the triple coincidence unit was used to gate the total energy signal (E_t=ΔE+E'+E), the TAC signal, and supplied a trigger pulse to the data acquisition system. This gating scheme effectively rejected the

overwhelming background.

The conversion gains of the energy channels were set and monitored by detecting alphas from ^{241}Am sources. The procedure for adjusting the channel settings was straightforward in principle but is infact nontrivial and required resetting after each run. Details can be found in Ref. 11.

C. Multiple Scattering

The major drawback of using the coincidence technique to extract the events of interest from the background was the lower count rate and the uncertainty regarding the detection efficiency. A measurement (at 29 MeV ^{3}He) of the number of genuine deuterons recorded with a particle telescope set at 25°, where the background was negligible, showed that there were 50% fewer counts when the same measurement was made requiring a coincidence with the recoil alphas. The main source of this discrepancy was multiple scattering in the target. The coincidence efficiency was reduced by the loss of those events, where one of the pair of particles was not detected. Geometrical effects were also found to be important. For instance, certain parameters, such as the diameters of the detector collimators, beam movement on target, and the size of the bombarding beam, would significantly influence the possibility of detecting all the coincidences. The sizes of the effects to be expected in the experiment were investigated by a Monte Carlo simulation.[11,13] The results confirmed the coincidence detection efficiency behaves in a rather complicated manner. This affected the ^{3}H(^{3}He,^{2}H)^{4}He experiment in two ways. First, the extraction of reliable correction factors for multiple Coulomb scattering of

the incident beam and the recoiling particles in the target proved to be intractable. What would have been useful cross-section data for the lower energies could not be obtained. Secondly, when determining the analyzing powers, the angular range over which the measurements could be confidently compared is restricted by the need to alter the target set-up to measure some angles and the lack of time to do intercomparison measurements. The data taken at 33 MeV and the forward-angle data taken at other energies were measured independently using left and right counters and therefore should be free of systematic errors. It is conceivable that a combination of effects like beam steering associated with change of polarization state could have influenced the coincidence data taken at the lower energies. The measured analyzing power angular distributions took many days to complete and, within statistical accuracy, we found no evidence to support this notion.

D. DATA REDUCTION

A typical TAC spectrum is shown in Figure 3a. The true coincidence peak is clearly resolved above the random coincidence background. This background is peaked at intervals of 83.2 ns, which corresponds to the repetition period of the cyclotron beam. The number of counts associated with the "true plus random" peak was corrected by subtracting the average number of counts in the energy spectra associated with the "random" peaks. All energy spectra were labelled and stored automatically according to the spin state of the beam. The energy spectrum in Figure 3b depicts the uncorrected, $^{3}H(^{3}He,^{2}H)^{4}H$ total-energy peak. There is very little relevant background. In this instance, a straightforward integration of the peak was made before calculating the analyzing power in the usual way.

E. RESULTS AND DISCUSSION

The measured analyzing powers are shown in Figure 4. A measure of confidence in our experimental technique can be gained from examining Figure 5, where the Birmingham measurements at 18 MeV are compared with the 17 MeV triton measurements reported by Haglund et al.[3] The expected agreement between the two sets of results is evident, and the data confirm the previous observation that the analyzing powers show pronounced deviations from antisymmetry.

Inspection of the data shows several other features. The analyzing power at 33 MeV is almost antisymmetric, as would be expected from isospin considerations. However, the measurements made for 29 MeV show the analyzing powers start to differ from this antisymmetry but still cross zero at 90°. At 27 MeV, a slight deviation from cross-over at 90° is observed, and the backward-angle analyzing powers ($\geq 90^{o}$) are reduced in magnitude compared with the complementary forward-angle ones. Below 24 MeV the zero crossing point has shifted to an angle much less than 90° and continues to shift with decreasing energy. In fact, the new data reveal a perceptible non-zero analyzing power at 90° only for incident ^{3}He beam energies below 24 MeV. This suggests that a Conzett-type model might be tenable at high energies and could even actually predict the results. Another feature worth noting is that the analyzing powers in the angular range 70° to 90° cm have progressively decreased in magnitude with decreasing energy, and by 20 MeV the analyzing powers are just positive around 90° cm. At 18 MeV, however, they begin to increase in magnitude again, and this upward trend is confirmed by the low energy measurements of Haglund et al. at 17.02, 12.86, and 9.02 MeV.

The only reliable cross-section angular distribution measured in this experiment over a more or less complete angular range was that measured at 33 MeV beam energy. The yields at each angle were extracted and converted to center of mass cross sections. The normalization constant required to calculate the absolute cross sections was determined by comparing the nominal elastic tritium cross-sections which were also measured, with those of Vlastou et al.[12]. The 33 MeV cross sections are shown in Figure 7, where the error bars indicate the statistical uncertainties. There is a possible systematic error in the range $\pm 2.5\%$ arising from the uncertainty in the normalization constant.

A comparison between the cross-section measurements at $E(^3He)=33$ MeV and those calculated using the reciprocity relation and the inverse $^4He(^2H,^3H)^3He$ reaction data $\{E(^3He)=32.2$ MeV$\}$ reported by Roberts et al.[14] is shown in Figure 8. The overall agreement is satisfactory except in the angular range 60-120° cm, where the Birmingham cross-section measurements are smaller by almost 1 mb/sr. In the absence of other measurements at neighboring energies, it is difficult to assess whether or not the discrepancy arises from the energy dependence of the cross section. It remains true, however, that a set of accurate cross-section measurements is needed to go with the analyzing power measurements in order to perform a complete analysis of all data.

III. THE DWBA MODEL

The reaction, in its simplest form, is considered to proceed by a direct, single nucleon transfer mechanism. Because of the mass and isospin

identity of the incident channel particles, the reaction is described by the sum of amplitudes from the single proton and single neutron transfers at complementary angles and is depicted in Figure 6. For typographical convenience, consider a reaction of the simple form C'(C,A)B where C and C' are members of an isospin multiple (^{3}He and ^{3}H in our case), and suppose particle A is observed at a cm angle θ. The direct mode is represented by

$$C+C' = (A+n_1) + C' \rightarrow A+(C'+n_1) = A+B$$

whereas the exchange mode is

$$C+C' = C + (A+n_2) \rightarrow A + (C+n_2) = A+B$$

where n_1 and n_2 are the transferred (proton and neutron) particles.

In the first case, particle C is stripped, producing particle A at angle θ. The scattering amplitude describing this process is denoted β_1^{mba} (θ;C'(C,A)B). In the second case, particle C' is stripped producing particle B at $\pi-\theta$ and particle A recoils at the angle θ. The amplitude for this process is β_2^{mbc} ($\pi-\theta$;C'(C,B)A).

We treated this model in the exact finite range (EFR) DWBA. In the evaluation of the direct and exchange amplitudes, channel spin formalism, the usual method, was not used. Instead, the symmetry properties of the reaction were exploited to calculate the reduced amplitudes $\beta_{1,2}$, which are elements of the angular momentum transfer representation of the T-matrix[15]. The reason for choosing this method was solely the

availability of an exact finite range DWBA computer code, which included spin orbit coupling in the entrance and exit channels. The code FRUCK2 (ref 16) was adapted to output the single nucleon transfer, reduced amplitudes $\beta_{1,2}$ and other relevant information. A separate computer program was written to sum coherently the direct and exchange amplitudes and then to calculate the experimental observables. The formalism for adding the transition amplitudes is given in the literature[10,17] and details of our method are described elsewhere[11]. However, the logical basis of the method will be briefly expounded here. To simplify notation, let the intrinsic spin projections of the ^{3}He, ^{2}H, ^{3}H and ^{4}He be represented by the symbols a,b,c, and d respectively and define m=a-d since this quantity is actually used in the DWBA program to label the scattering amplitudes. The reduced amplitudes β_1^{mba} (θ) and β_2^{mbc} $(\pi-\theta)$ are calculated separately (using FRUCK2) as if they arose from single nucleon stripping by the projectile, that is from the ^{3}He or the ^{3}H, respectively. The direct and exchange processes are coherently summed by constructing the antisymmetric amplitude.

$$\beta_{anti}^{mba} = \beta_1^{mba}\ (\theta) + (-1)^{a-m-b}\ \beta_2^{mbc}\ (-\theta)$$

for each ℓsj transfer quantum numbers and outgoing partial wave L_b. In our particular case ℓ=0, s=1/2, j=1/2. The addition is possible because both sets of amplitudes, $\beta_1^{mba}(\theta)$ and $\beta_2^{mbc}(\pi-\theta)$, have corresponding 'like' labels. The phase difference arises from the change to a common frame of reference before the addition of amplitudes is carried out.

It is worth noting that the Conzett model assumes, on the basis of charge symmetry, that $\beta_1^{mba}(\theta) = \beta_2^{mbc}(\pi-\theta)$, and it is this condition which guarantees antisymmetric analyzing powers. The reason for this result can be traced to the cancellation of the direct and exchange amplitudes for all odd partial waves. However, in our analysis this assumption was not made because it is reasonable to expect that $\beta_1^{mba}(\theta)$ will differ slightly from $\beta_2^{mbc}(\pi-\theta)$ because of Coulomb-induced differences between the helion and the triton. These exist without necessarily implying charge symmetry violation by the nuclear interactions.

A systematic investigation of the factors which comprise the multi-dimensional DWBA integral and hence generate the reduced amplitudes was performed. In the post representation

$$\beta_{1,2}(\theta) \propto \int \chi^{(-)} \langle \phi_{pt} | V_{pd} \phi_{pd} \rangle \chi^{(+)} d\tau$$

for proton stripping. $\chi^{(-)}$ and $\chi^{(+)}$ are the outgoing and ingoing distorted waves. These were calculated after constructing, in the usual manner, an optical model potential by fitting the relevant elastic scattering data[12,18]. When fitting the $^2H+^4He$ channel, no serious attempt was made to use the tensor-analyzing power data. Table 1 lists the best fit Woods-Saxon parameters obtained after carrying out numerous two-parameter grid searches as well as using conventional search techniques. In the integral, ϕ_{pd} and ϕ_{pt} are the radial parts of the ^3He and ^4He bound state wave functions, and V_{pd} is the proton-deuteron binding potential. A

Woods-Saxon potential was also used when computing the bound state wave functions with its well depth adjusted to reproduce the separation energy. The bound state parameters used in the analysis are given in Table 1. In the corresponding exchange term a neutron is stripped from the ^3H, and the equivalent quantities are also listed in Table 1.

IV. DWBA ANALYSIS

The results of a single proton transfer calculation at 33 MeV incident energy are depicted in Figure 7. The fits to the data are very poor. The calculated cross section has the wrong shape and is almost a factor of ten too large, while the analyzing power is in antiphase with the experimental measurements. Also shown on the same figure are the predictions corresponding to a neutron pickup from the target. The calculated differential cross section is almost identical to that obtained in the stripping calculation and the analyzing powers, although now in phase with the data, still fail to reproduce the details. In fact, a close examination reveals that the results are simply mirror images of each other about 90°. In the next calculation the stripping and pickup-reduced amplitudes were combined coherently in accordance with the procedure outlined above. The results at 33 MeV are shown in Figures 8 and 9. The analyzing power calculations are portrayed as a function of entrance channel spin-orbit strength (V_{so}=0.1 MeV and V_{so}=1.5 MeV). The fit to the experimental data is very good, and zero vector analyzing power at 90° cm is predicted. The interesting observation is that the analyzing power predictions are more or less antisymmetric except for the slight fore-aft deviation from antisymmetry near the cross section minima at

60° and 120° cm. Also, there are very minor differences between the calculated results shown in Figure 8 and a prediction obtained using the Conzett model; that is, a model explicitly requiring $\beta_1^{mba}(\theta)=\beta_2^{mbc}(\pi-\theta)$. Evidently, effects arising from Coulomb differences in the bound states of the ^3He, ^3H and ^4H nuclei are marginal. Therefore, Coulomb differences alone cannot be directly responsible for the observed non-zero 90° cm analyzing power with incident beam energies below 24 MeV and particularly those at 18 MeV. However, the good fit does comfirm the validity of the model and the assumptions embodied therein. Moreover, there is no evidence at high energies to support an argument for charge symmetry violation.

To construct the lower part of Figure 8, the $^4He(^2H,^3H)^3He$ cross sections of Roberts et al.[14] and semi-detailed balance were used to calculate the angular distribution of the fore-aft asymmetry parameter $R(\theta)$. This is defined as the ratio of yield of ^3H at θ_{cm} and ^3H at $(\pi-\theta)$ cm; that is, $R(\theta)=\sigma_{3H}(\theta)/\sigma_{3He}(\theta)$. It is clear from Figure 4 that there are deviations of up to 20% from the predicted symmetry in the cross sections and, therefore, it is important to see whether our DWBA model can explain this behavior. The result of the DWBA computation is shown on the same figure. The agreement between the theoretical curve and the experimental measurements is good, and the calculation is able to account for both the magnitude and shape of the asymmetry in the angular range $30^o<_{cm}\theta<150^o$. A closer examination shows that large asymmetries are always associated with a minimum in the differential cross sections. Since the minima are the result of the cancellation of the $\beta_1^{mba}(\theta)$ and $\beta_2^{mbc}(\pi-\theta)$ amplitudes, such differences are to

be expected because it is near these minima that the sensitivity to small differences between $\beta_1(\theta)$ and $\beta_2(\pi-\theta)$ is the largest. The over-predictions, or "spikes," at larger forward and backward angles occur at the first minimum (22.5^o), while the 20% difference mentioned above is located at the second minimum (62.5^o). Although Coulomb differences between various bound states give rise to slightly different β_1 and β_2 amplitudes, these amplitudes are also influenced by the other factors in the DWBA overlap integral that generates them. That is, there is an intricate relationship between the predicted deviations from symmetry and the many dynamical factors of the reaction. Detailed analysis strongly suggests that previous observations of asymmetry in the $^4He(^2H,^3H)^3He$ cross sections[1,14] can be adequately explained by reaction dynamical effects.

The results from similar coherent sum DWBA calculations at 18 MeV incident energy are depicted in Figure 10 together with the new polarized ^3He data and the 17 MeV polarized triton measurements of Haglund et al. The agreement between experiment and theory is again satisfactory, but the most striking result is the observed variation of the calculated 90° analyzing power with the strength of the spin orbit interaction in the entrance channel. It is at first surprising to find that not only does the 90° cross-over point move towards a smaller angle with increasing V_{so}, but also that it reaches a cross-over position which corresponds almost exactly to the measured value (80° cm) at the expected value of V_{so}. Any further increase in V_{so} shifts the cross-over point back to 90° cm. The optimum and reasonable value of V_{so}=1.5 MeV seems to reproduce the anomalous behavior of the vector analyzing powers at 18 MeV. Moreover, a general

feature of all calculations performed so far is that, except for a narrow range ($\pm$2 MeV) of incident ^{3}He energies centered about 18 MeV, the 90° cm analyzing power predictions are zero and are insensitive to the strength of the spin orbit potential in either the entrance or the exit channel. It is noted that the prediction of deviation from 90° cross-over in the ^{3}He or ^{3}H analyzing powers implies a similar, but smaller, deviation in the deuteron vector analyzing power for the inverse reaction.

V. RESONANCES

The only possible energy-dependent difference between the two sets of DWBA calculations (i.e., at 33 MeV and 18 MeV incident energy) must relate to the distorted waves. A careful scrutiny of the calculated elastic scattering S-matrix elements identified a resonance in the $F_{7/2}$ entrance channel partial wave. This leads to the internal wave function reaching a maximum which is comparable in magnitude with the wave function in the external region as illustrated in the lower part of the Figure 11. The optical potential resonance was easily identified by the characteristic counterclockwise trajectory on an Argand plot of the real and imaginary phase shifts. The latter phase shifts reproduced reasonably well the phase shifts determined by Vlastou-Zannis et al.[12] from an analysis of the ^{3}He+^{3}H elastic scattering data. The resonance energy was determined to be 18 MeV (E_x in ^{6}Li=24.8 MeV). The width Γ of the $F_{7/2}$ resonance was obtained by calculating complex eigenstates in the optical model potential using the computer code GAMOW[19]. A value of Γ in the range $2.6<\Gamma<3.4$ MeV was deduced. In addition, the calculations showed no other nearby potential resonances.

However, the resonance on its own would not explain the calculated deviation from 90° cm cross-over, because the distorted waves appear in both the direct and exchange computations. The complete explanation must involve the bound state formfactors, which are of course independent of energy. The upper part of Figure 11 shows the clear disparity at short range (r<1.5 fm) between the ^{3}He ($V_{pd}|\phi_{pd}>$) and ^{3}H ($V_{nd}|\phi_{nd}>$) form factors used to evaluate the proton stripping (direct) and neutron stripping (exchange) transition amplitudes. The difference between the n+^{3}He and p+^{3}H bound state wave functions is negligible and is not illustrated here. The conclusion that genuine physical differences between the ^{3}He and ^{3}H wave functions exist is supported by the results of Ioannides et al[20], who calculated the $<^{3}He|d>$ and $<^{3}H|d>$ overlap functions using the Phillips tri-nucleon wave functions. Barshay and Seghal[21] proposed a simple geometrical model to explain the difference in the distribution of matter in tri-nucleon systems. The model assumed a short-ranged three-nucleon correlation, which is a symmetrical triangular configuration in the ^{3}H nucleus; whereas in the ^{3}He nucleus the triangle was distorted by the Coulomb repulsion of the protons. Very recently, Friar et al.[22] have reported on the sensitivity of tri-nucleon densities to effects of the pp Coulomb interaction in ^{3}He ground state. Their investigation and the Barshay-Sehal model predict differences of the type shown in Figure 11. Ordinarily the differences between the tri-nucleon form factors are not significant as shown by the results of the DWBA computations at 33 MeV. However, the occurrence of a strong potential resonance magnifies the effects of the short range differences, and this can be seen when the DWBA overlap

integral is calculated. Particularly, the inequality between the L_b=3, direct ($\beta_1(\theta)$) and the exchange (π-θ) amplitudes is sufficient to admit a sizeable odd L component to the total scattering amplitude because of incomplete cancellation. This is manifested in the final prediction as a non-zero analyzing power at 90^0 cm (i.e., as deviations from antisymmetry). The sensitivity to the entrance channel spin-orbit potential (V_{so}) or the incident beam energy, is understood as both quantities strongly influence the resonance amplitude. It should be emphasized that within the framework of our DWBA model the shifts away from 90^0 cm cross-over are the signatures of odd L-wave resonances only. The concern with odd L-wave admixtures does not arise when isolated positive parity resonances are considered, and therefore the appropriate symmetries in the observables are expected. If in reality there exist positive parity states, there is a risk of being oblivious to their presence unless a very careful analysis is carried out.

The calculations did not fully include the effects of the target spin because the DWBA code FRUCK2 assumes zero target spin. Consequently, the spin parity (J) of the entrance channel resonance was not fully determined. However, Weller et al.[23)] studied the theory of spin 1/2 on spin 0 and spin 1/2 on spin 1/2 scattering systems in order to find what relations between the scattering phase shifts in the two systems were necessary in order to yield identical calculated values of the observables. For the spin 1/2 on spin 1/2 scattering the channel spin formalism was employed including the possibility of singlet-triplet mixing, but excluding L-mixing. The relations found

between the spin 1/2 on spin 0 phases ($\delta^{\pm}$) and the spin 1/2 on spin 1/2 phases ($\delta^{J}LS$) are as follows:

$$\delta_L^- = \delta_{L1}^{L}, \ \delta_L^- = \delta_{L1}^{L-1}, \ \delta_L^+ = \delta_{L0}^{L}, \ \delta_L^+ = \delta_{L1}^{L+1}$$

These relations provide some guidance in deciding which partial waves are likely to be found to be resonant if a proper spin 1/2 on spin 1/2 analysis was made. In particular, the $F_{7/2}$ resonance found in our analysis would correspond to either a $^{11}F_3$ ($^{2T+1,2S+1}L_J$) or a $^{33}F_4$ resonance in the compound ^{6}Li system. The latter possibility can be rejected because $\Delta T=1$ transitions are isospin forbidden. Therefore, it seems very likely that the $F_{7/2}$ resonance corresponds to a $J=3^-$, T=0 level at 24.8 MeV excitation in ^{6}Li. Given the dominance of the F wave process it is deduced from general isospin and parity considerations that the reaction near 18 MeV should proceed via the $^{11}F_3(^3He+^3H) \rightarrow$ $^{13}F_3(^3H+^4He)$ isospin allowed (T=0) transition.

Vlastou et al.[12] carried out a phase shift analysis of the $^3He+^3H$ elastic scattering data with proper attention given to antisymmetrization and found evidence for a 3^- T=0 state at 25 MeV excitation in ^{6}Li. One analysis of the data included only real phase shifts for partial waves up to L=4 and no coupling parameters. A more realistic analysis with complex phase shifts and mixing parameters was also completed. An examination of the two sets of phase shifts (particularly the extra imaginary phase shifts) revealed the expected minor differences and enabled them to deduce which resonances feed the elastic channels. The main

difference between the two solutions is in the $^{11}F_3$ (T=0) phase shift, which is negative and structureless in the first case, but positive and showing resonance behavior in the second. It is postulated that most of the strength of the $^{11}F_3$ resonant state decays through a reaction channel, but because the $^3H(^3He,d)^4He$ reaction data were not available to Vlastou et al, they could not verify that this was the relevant channel.

Jenny et al[24] have reported the results of a very detailed phase shift analysis of $d+^4He$ elastic scattering in the energy range 3 to 43 MeV. They report the existence of a $^{13}F_3$ (T=0) resonance centered at E_x=24 MeV in ^6Li, which they suggest corresponds to a broad 3^- state at E_x=26.6 MeV in the ^6Li level scheme[25]. There is considerable uncertainty regarding the state at E_x=26.6 MeV because Vlastou et al clearly identify this as a T=1 state. The assignment shown in the ^6Li level scheme is only tentative, since it is based on the poor statistics $^3H(^3He,\gamma)^6Li$ measurements of Ventura et al[26].

The evidence from both the $^3He+^3H$ and $d+^4He$ elastic phase shift analyses, from the analyzing power measurements and our analysis discussed above strongly suggest the existence of a broad $J=3^-$,T=0 level in ^6Li at E_x=24.8 MeV with $\Gamma\simeq3$ MeV.

VI. SUMMARY AND CONCLUSION

Vector analyzing powers for the $^3H(^3He,d)^4He$ reaction have been measured over an incident beam energy range 18-33 MeV. For energies above 24 MeV, the analyzing powers are almost antisymmetric and cross zero at 90°. The experimental data are satisfactorily reproduced by DWBA calculations

assuming a Conzett-type reaction mechanism. The gross deviation from anti-symmetry at 18 MeV and in particular the large negative analyzing power at 90° are explained by the existence of a $J=3^{-}$ $T=0$ resonance in ^{6}Li, which magnifies the effects of short-range Coulomb-induced differences between the ^{3}He and ^{3}H nuclei. This prevents the cancellation of an odd partial wave in the total transition amplitude and results in predicted deviations from antisymmetry. Because this mechanism is purely dynamical, the results provide no evidence in support of charge symmetry violation.

It is our pleasure to thank Professor G. C. Morrison for his continuing interest and support. Our warmest thanks go to Dr. R.F. Haglund (Los Alamos) for sending us the polarized triton data and Professor S.E. Darden (Notre Dame) for reading this paper and making helpful comments. We acknowledge the support of the Science and Engineering Research Council (SERC), U.K. which facilitated this work.

*This work was partially supported by the Director, Office of Energy Research, Division of Nuclear Physics of the Office of High Energy and Nuclear Physics of the U.S. Department of Energy under Contract DE-AC03-76SF00098.

Table 1. Optical Model and Bound State Parameters used in the DWBA calculations

All optical model parameters have been converted to the form of the potential V(r) used in FRUCK2.

$$V(r) = V_R f(r,r_R,a_R) + iV_I f(r,r_I,a_I) + iV_I' a_I' \frac{df}{dr}(r,r_I',a_I') + V_{so}\frac{1}{r}\frac{df}{dr}(r,r_{so},a_{so})L.S$$

where the Woods-Saxon well is given by

$$f(r,r_i,a_i) = \left[1 + \exp\left[\frac{r - r_i A^{1/3}}{a_i}\right]\right]^{-1}$$

and A is the target mass

Energy	Channel	V_R (MeV)	r_R (fm)	a_R (fm)	V_I, V_I' (MeV)	r_I (fm)	a_I (fm)	V_{so} (MeV fm^2)	r_{so} (fm)	a_{so} (fm)
33.0 MeV	^{3}He+^{3}H	-202.8	1.52	0.18	-1.06*	4.20	0.50	-6.0	0.83	0.10
	^{2}H+^{4}He	-63.0	1.18	0.56	-14.80**	2.56	0.50	-9.2	1.18	0.50
18.0 MeV	^{3}He+^{3}H	-199.9	1.57	0.18	-0.92*	2.34	1.43	-6.0	0.73	0.10
	^{2}H+^{4}He	-67.3	1.18	0.56	-11.20**	1.00	0.50	-9.2	1.18	0.50

Separation Energy	Bound State	V_R (MeV)	r_R (fm)	a_R (fm)	Separation Energy	Bound State	V_R (MeV)	r_R (fm)	a_R (fm)
-19.81	p+^{3}H	-71.48	1.25	0.65	-5.49	p+^{2}H	-51.84	1.25	0.65
-20.58	n+^{3}H	-79.60	1.25	0.65	-6.26	n+^{2}H	-58.38	1.25	0.65

*Volume Imaginary Potential V_I; **Surface Imaginary Potential V_I'

Coulomb radius $r_c = 1.3\ A^{1/3}$ fm.

REFERENCES

1. E.E. Gross, E. Newman, M.B. Greenfield, R.W. Rutkowski, W.J. Roberts, and A. Zucker, Phys. Rev. C5, 602 (1972).

2. W. Dahme, H.E. Conzett, J. Arvieux, J. Birchall, and R.M. Larimer, Proc. 4th Int. Symp. on Polarization Phenomena in Nuclear Reactions, Basel, edited by W. Gruebler and V. Konig (Birkhauser, Basel, 1976), p. 497.

3. R.F. Haglund, Jr., G.G. Ohlsen, R.A. Hardekopf, Nelson Jarmie, and Ronald E. Brown, Phys. Rev. C16, 2151 (1977).

4. S. Barshay and G.M. Temmer, Phys. Rev. Lett. 12, 728 (1964).

5. H.E. Conzett, Proc. 4th Int. Symp. on Polarization Phenomena in Nuclear Reactions, Basel, edited by W. Gruebler and V. Konig (Birkhauser, Basel, 1976), p. 105. See also reference 8 below.

6. R.H. Drachman, Phys. Rev. Lett. 17, 17 (166).

7. U. Nocken, U. Quast, A. Richter, and G. Schrieder, Nucl. Phys. A213, 97 (1973).

8. A. Richter and C.M. Vincent, Phys. Rev. Lett. 25, 1460 (1970).

9. Michael F. Werby and D. Robson, Nucl. Phys., A234, 346 (1974).

10. Steve Edwards, D. Robson, Thurman L. Talley, William J. Thompson, and Michael F. Werby, Phys. Rev. C8, 456 (1973).

11. G. Rai, Ph.D. thesis, University of Birmingham, England, unpublished (1985).

12. R. Vlastou-Zannis, J.B.A. England, O. Karban, and S. Baird, Nucl. Phys. A292, 29 (1977).

13. G. Rai, Multiscatt - A program for calculating coincidence counting rates using the Monte-Carlo Method, University of Birmingham, Dept. of Physics report 84-05, unpublished.

14. W.J. Roberts, E.E. Cross, and E. Newman, Phys. Rev. C9, 149 (1974).

15. G.R. Satchler, Nucl. Phys. A55, 1 (1964).

16. Program FRUCK2, P.D. Kunz (unpublished); extended version of J.R. Comfort (unpublished) 1983.

17. W. Tobocman, Theory of Direct Nuclear Reactions, Oxford University Press, 1961; M.A. Nagarajan and M.K. Banerjee, Nucl. Phys. 17, 341 (1960); S. Edwards, Nucl. Phys. 47, 652 (1963).

18. E.J. Stephenson, H.E. Conzett, R.M. Larimer, B.T. Leemann, R. Roy, and P. von Rossen, Phys. Rev. C21, 44 (1980).

19. T. Vertse, K.F. Pal, and Z. Balogh, Comp. Phys. Comm. 27, 309 (1982).

20. A.A. Ioannides, M.A. Nagarajan, and R. Shyam, Nucl. Phys. A365, 150 (1981).

21. S. Barshay and L.M. Seghal, Phys. Rev. C31, 2133 (1985); see also S. Barshay, Prog. Theo. Phys. 74, 1077 (1985).

22. J.L. Friar, B.F. Gibson, G.L. Payne, Phys. Rev. C35, 1502 (1987).

23. H.R. Weller, J. Szucs, P.G. Ikossi, J.A. Kuehner, and D.T. Petty, Phys. Rev. C18, 1120 (1978).

24. B. Jenny, W. Gruebler, V. Konig, P.A. Schmelzbach, and C. Schweizer, Nucl. Phys. A397, 61 (1983).

25. F. Ajzenberg-Selove, Nucl. Phys. A413, 1 (1984).

26. E. Ventura, C.C. Chang, W.E. Meyerhof, Nucl. Phys. A173, 1 (1971).

Figure Captions:

Figure 1. The experimental setup for the coincidence measurements. Polarized ^{3}He beam enters the scattering chamber and interacts with the tritrium target. The beam polarization is monitored in the polarimeter chamber located downstream by measuring the left-right asymmetry of elastically scattered ^{3}He from a thin strip of deuterated polyethylene.

Figure 2. The mass and deuteron energy spectrum obtained using the ΔE-E telescope arrangement at 33 MeV incident ^{3}He beam energy.

Figure 3. Upper: A Typical TAC spectrum showing the random and true coincidence peaks. Lower: the deuteron energy spectrum associated with the true coincidence TAC peak.

Figure 4. Analyzing power angular distributions for the ^{3}H(^{3}He,^{2}H)^{4}He reaction measured at ^{3}He incident energies of 33,29,27,24,20 and 18 MeV. The error bars reflect the statistical uncertainty.

Figure 5. A comparision between the measured (crosses) 18 MeV ^{3}H(^{3}He,^{2}H)^{4}He and 17 MeV (solid squares) ^{3}He(^{3}H,^{2}H)^{4}He analyzing powers. The arrows indicate the crossover angle (θ_{cm} = 80°) at zero vector analyzing power.

Figure 6. Schematic diagram of the stripping and pickup components in a one step direct transfer model. The reduced transition amplitudes $\beta_{1,2}$() and the symbols are defined in the text.

Figure 7. DWBA calculations of the ^{3}H(^{3}He,^{2}H)^{4}He vector analyzing powers and cross-sections at 33 MeV assuming only a) stripping, and b) pickup, components of the reaction.

Figure 8. Coherent sum DWBA calculations at 33 MeV incident ^{3}He beam energy for the differential cross-section (upper) and asymmetry parameter R(θ) (lower). The Oakridge data is taken from ref. .

Figure 9. Coherent sum DWBA calculations ($E_{^3He}$ = 33 MeV) of the analysing power (upper) and differential cross-section (lower) as a function of the entrance channel spin orbit strength V_{so}.

Figure 10. Coherent sum DWBA calculations ($E_{^3He}$ = 18 MeV) as a function of V_{so}. The calculations predict a large deviation from zero analyzing power at θ_{cm} = 90° only if V_{so} = 1.5 MeV.

Figure 11. upper: The radial dependence of the ^3He and ^3H bound state factors used in the DWBA calculations.

lower: The radial dependence of the real part of the L = 3, J = 7/2, and 5/2 partial waves in the $^3He + ^3H$ entrance channel. The large internal $F_{7/2}$ amplitude reflects the resonance at $E_{^3He} = 18.0$ MeV, $V_{so} = 1.5$ MeV.

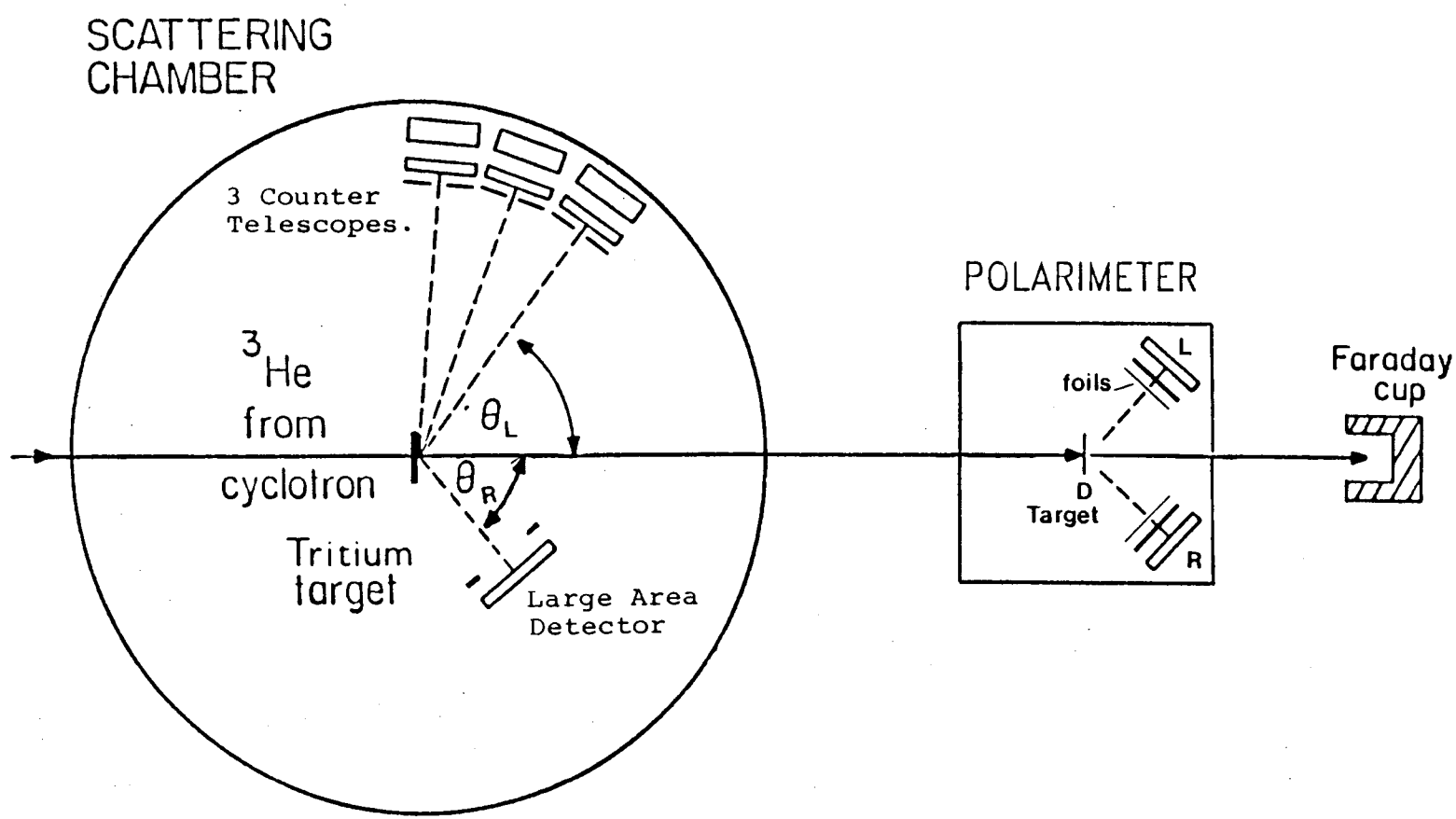

XBL 8711-5015

Fig. 1

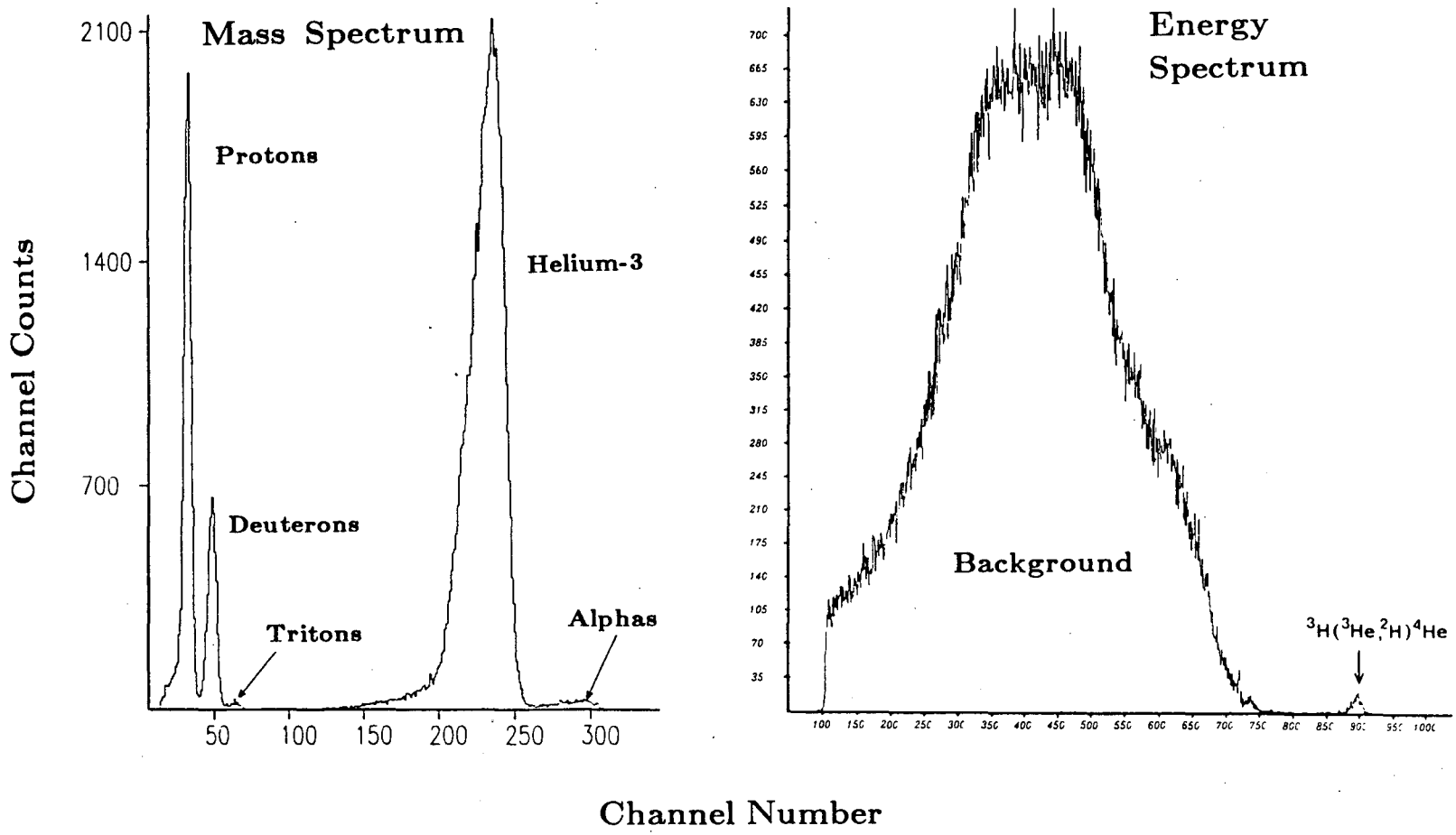

Fig. 2

XBL 8711-5016

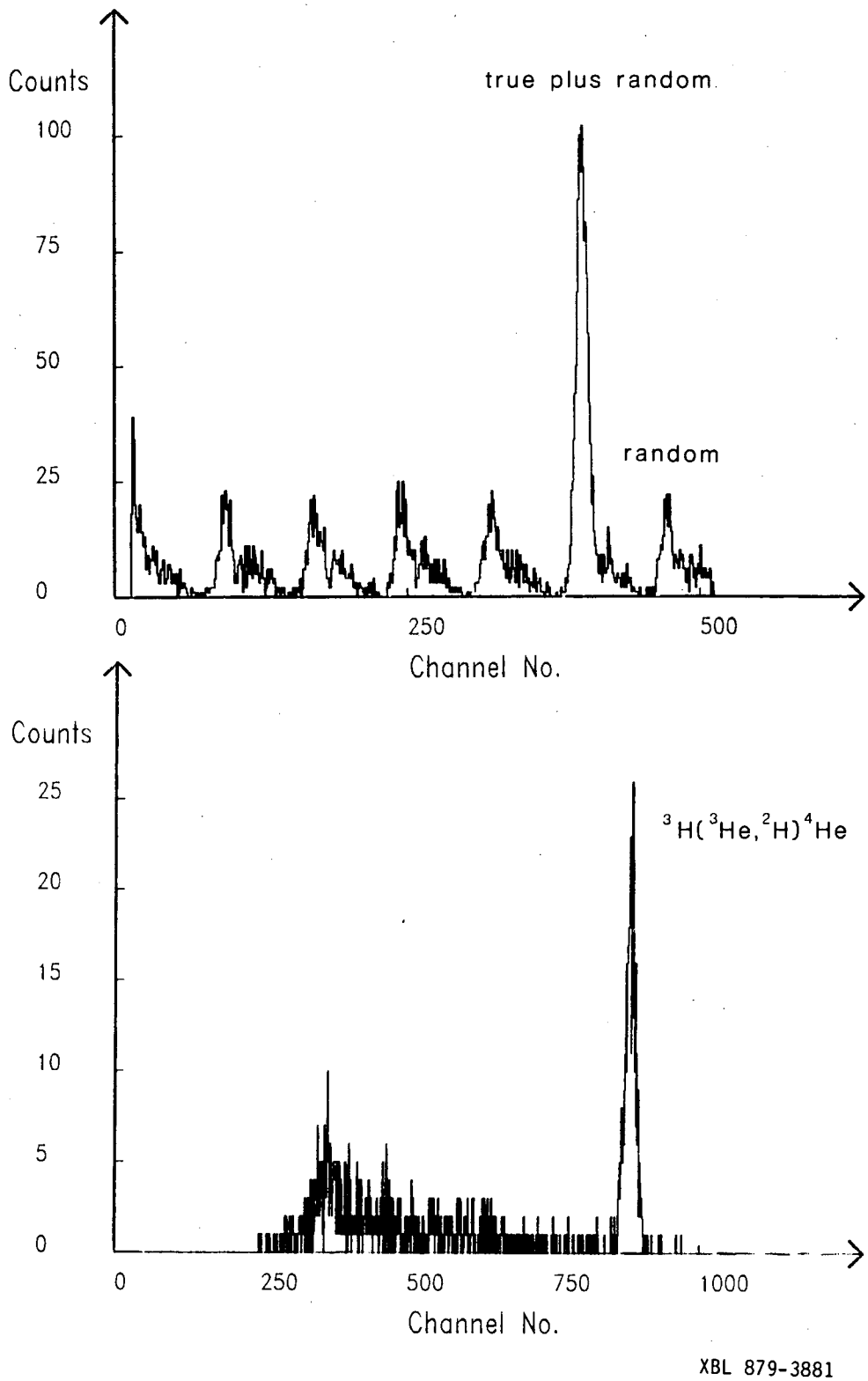
Counts
100
75
50
25
0
true plus random
random
0
250
500
Channel No.
Counts
25
20
15
10
5
0
$^3H(^3He,^2H)^4He$
0
250
500
750
1000
Channel No.
XBL 879-3881

Fig. 3

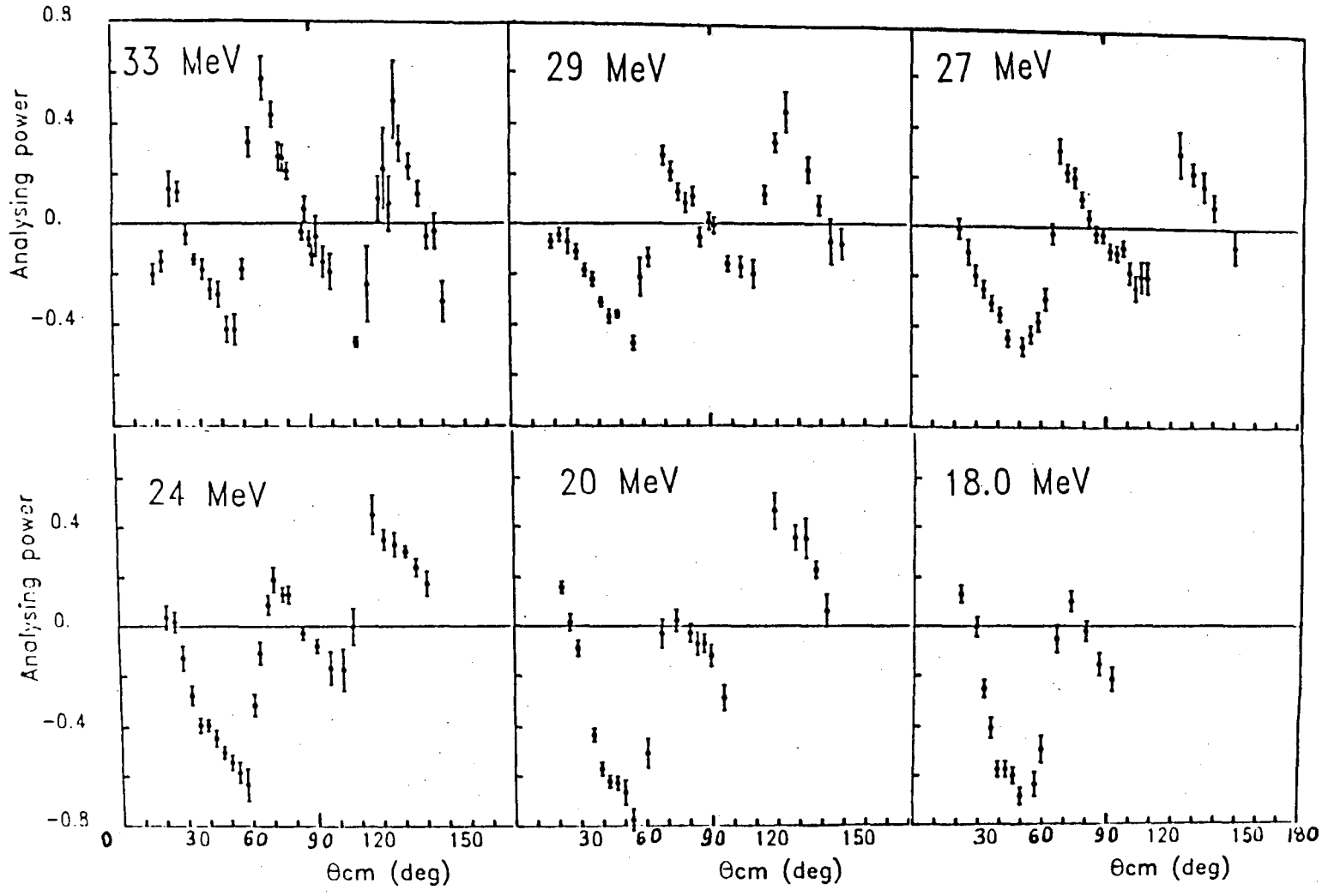

XBL 8711-5017

Fig. 4

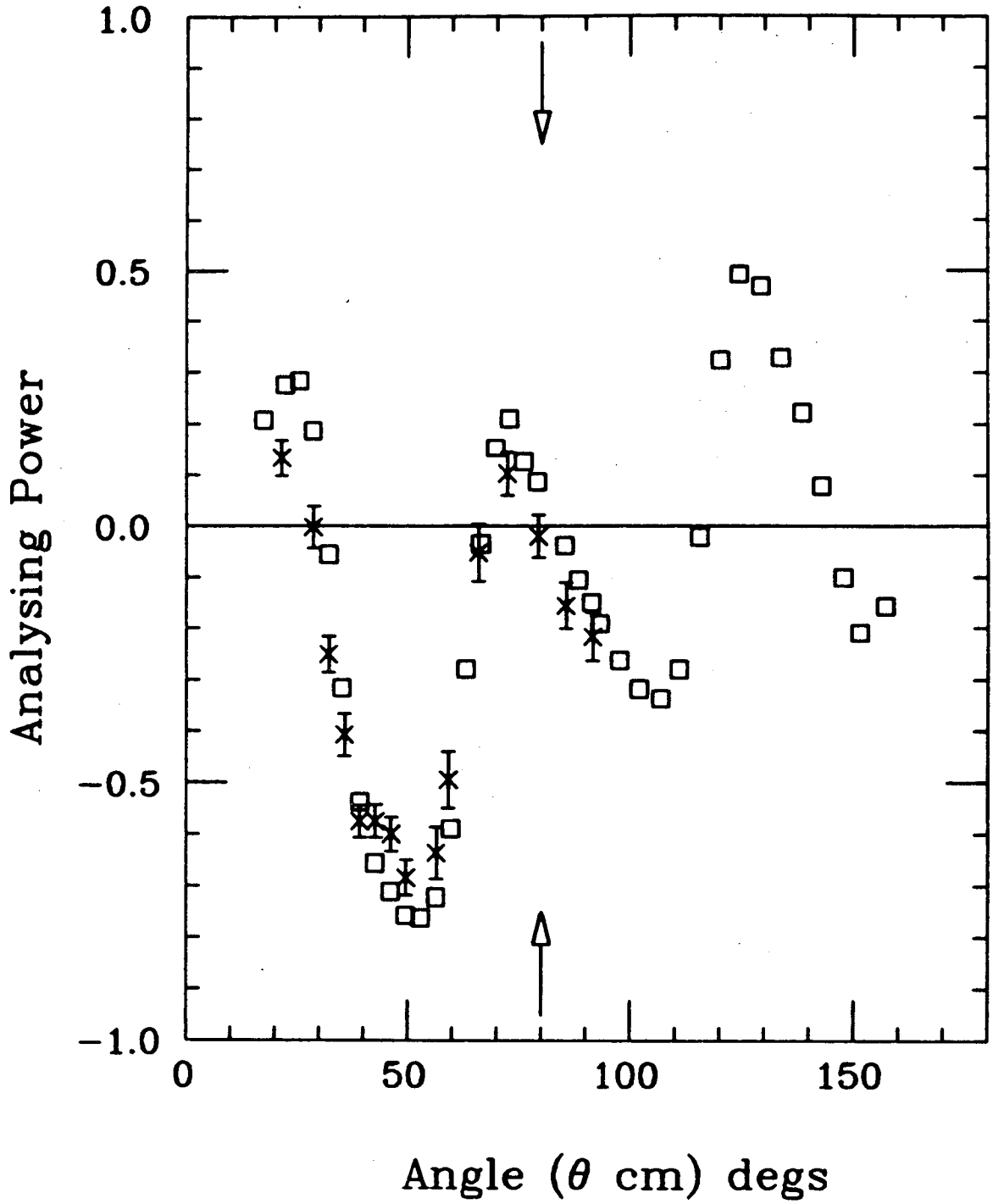

Fig. 5

XBL 8711-5018

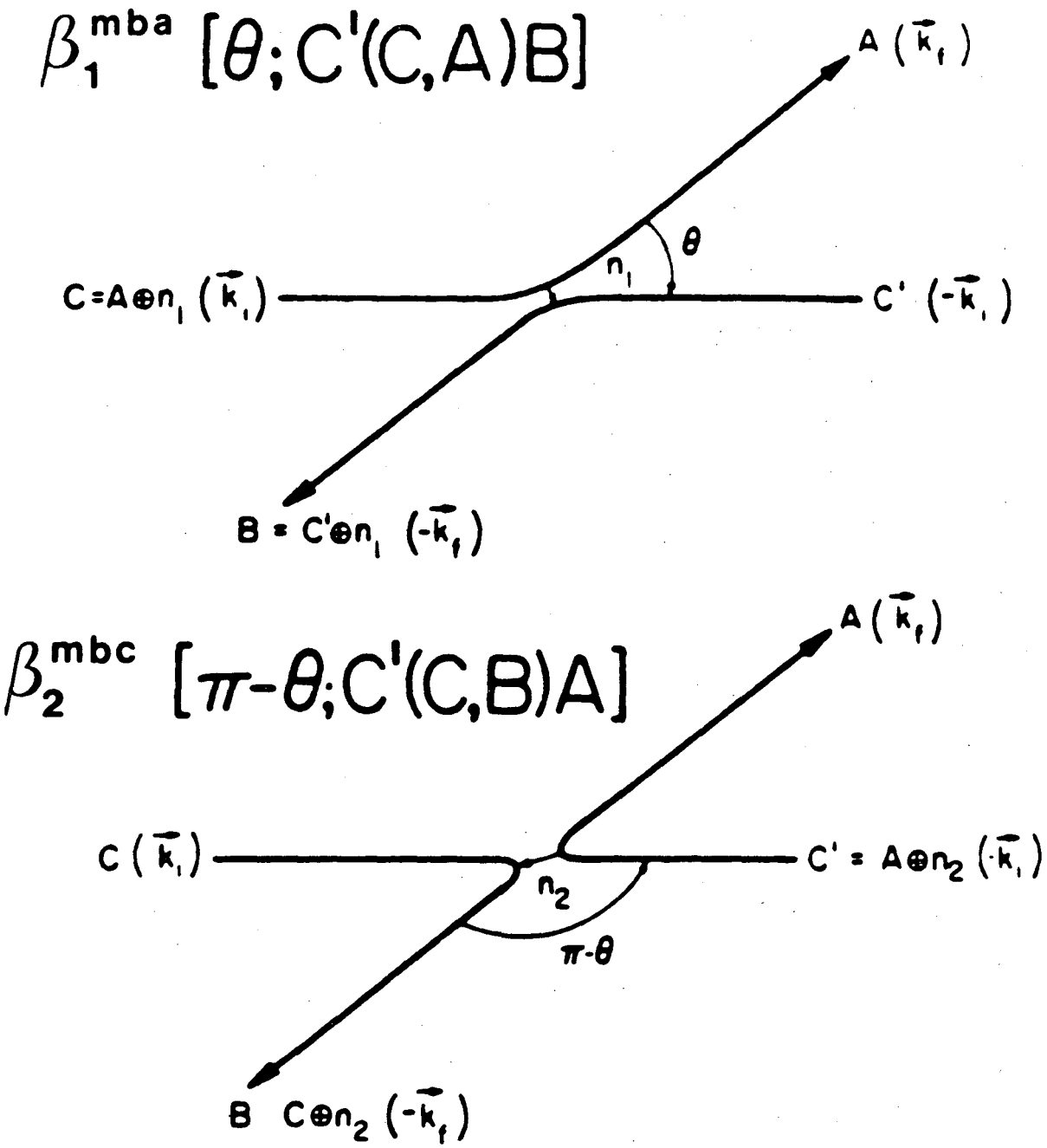

XBL 8711-5019

Fig. 6

$^3H(^3HE,^2H)^4HE$ AT 33.2 MeV INCIDENT ENERGY

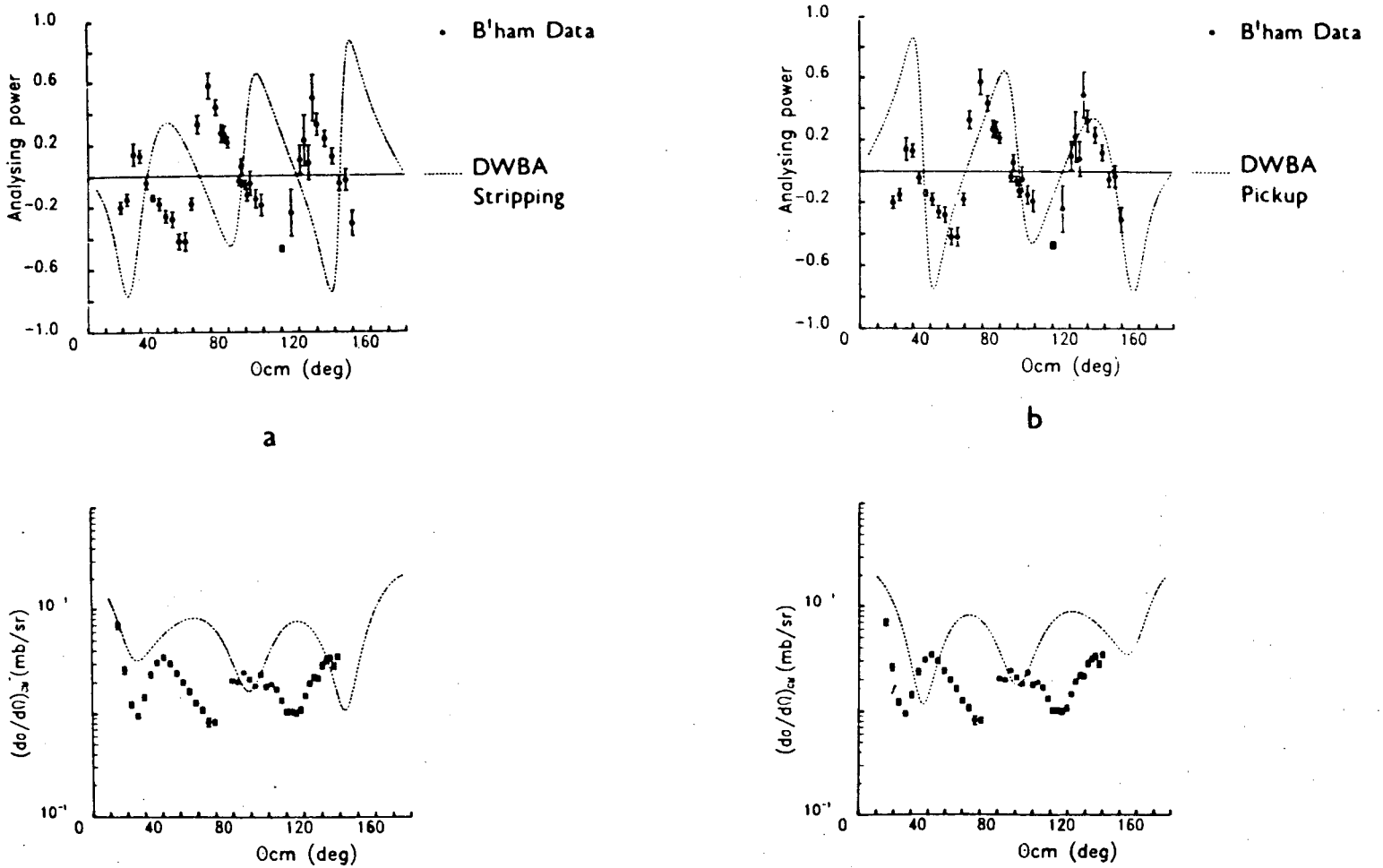

XBL 8711-5020

Fig. 7

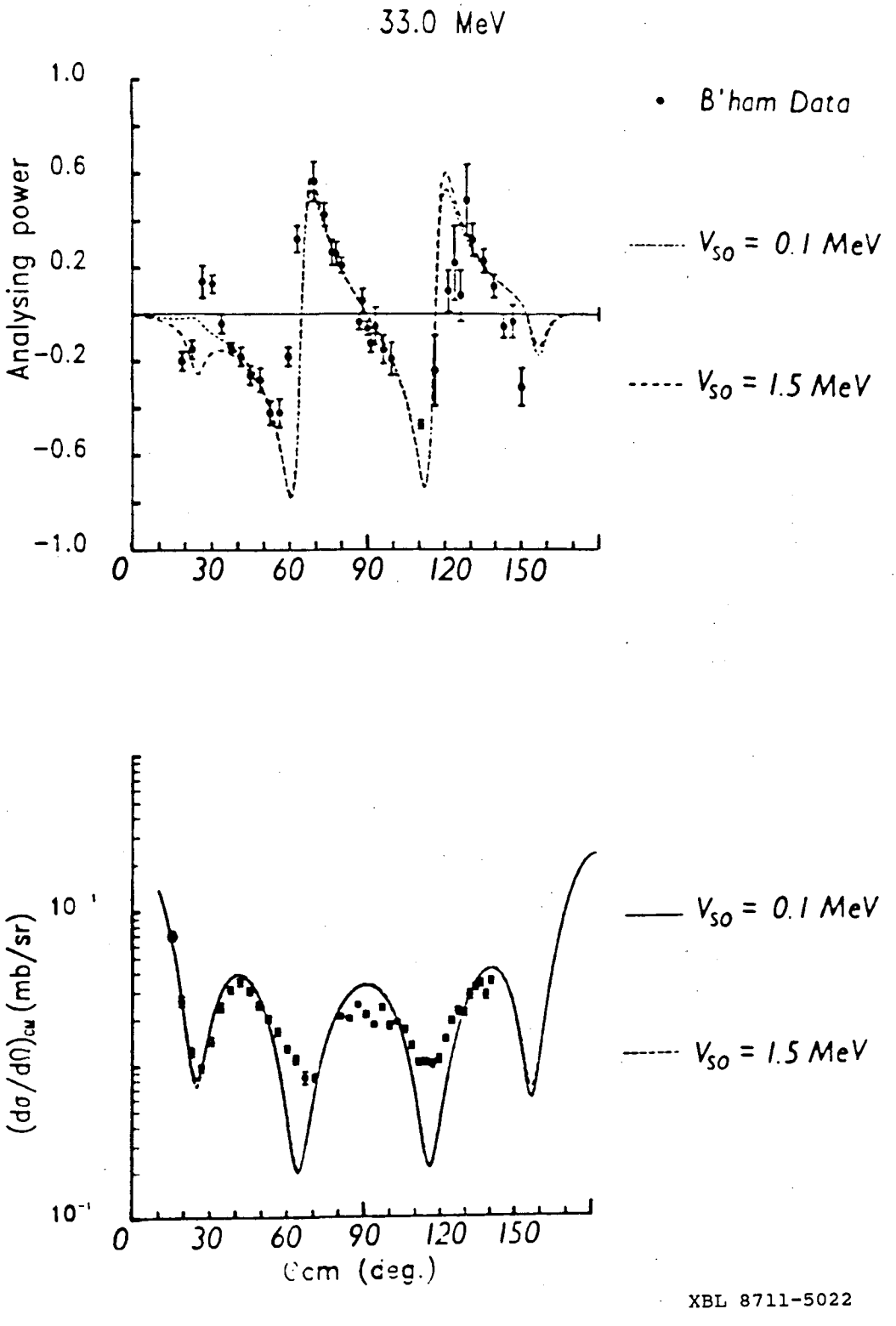
33.0 MeV
Analysing power
1.0
0.6
0.2
−0.2
−0.6
−1.0
0
30
60
90
120
150
• B'ham Data
V_{so} = 0.1 MeV
V_{so} = 1.5 MeV
$(d\sigma/d\Omega)_{cm}$ (mb/sr)
10^{1}
10^{-1}
θcm (deg.)
V_{so} = 0.1 MeV
V_{so} = 1.5 MeV
XBL 8711-5022

Fig. 8

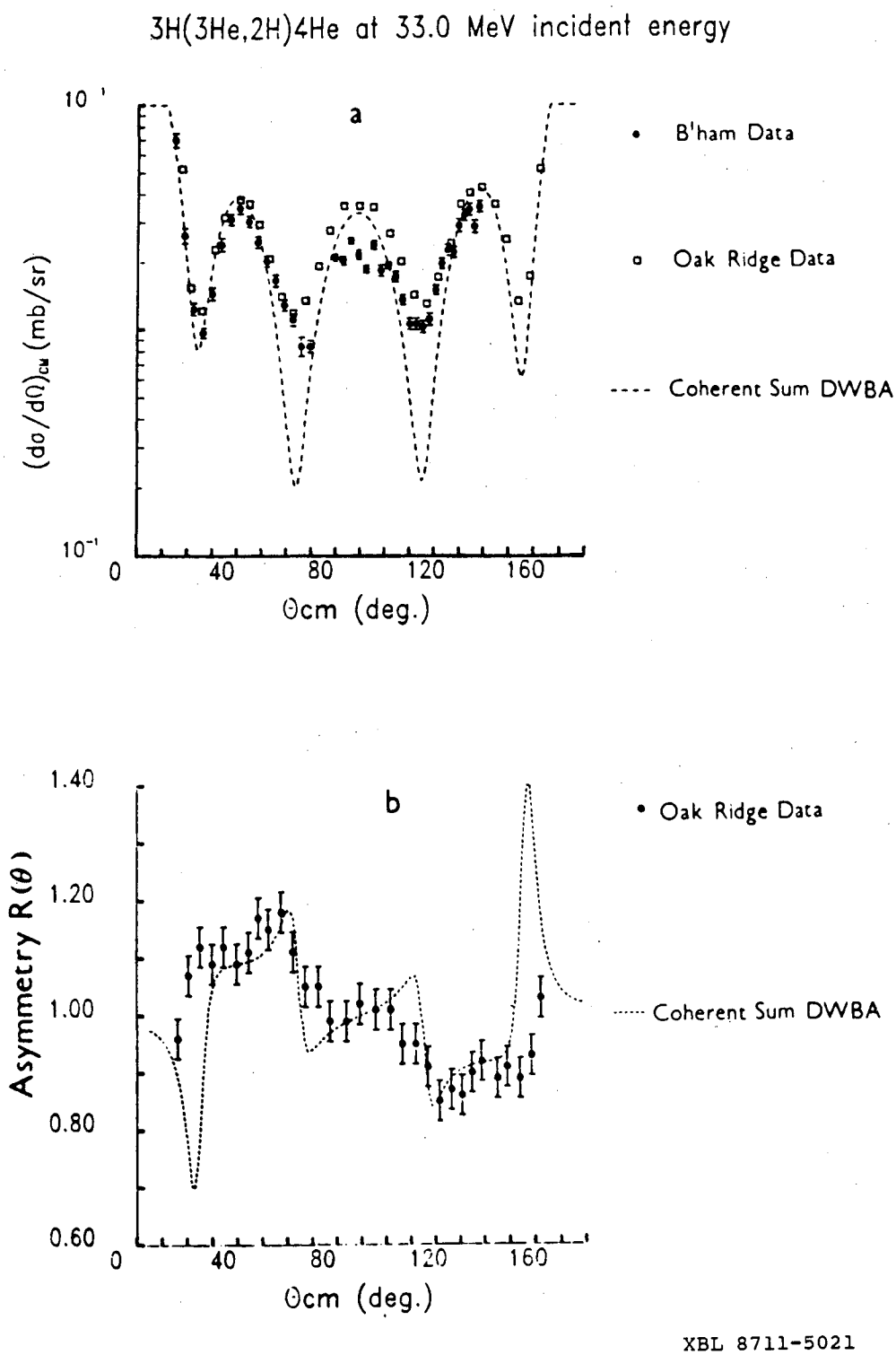

XBL 8711-5021

Fig. 9

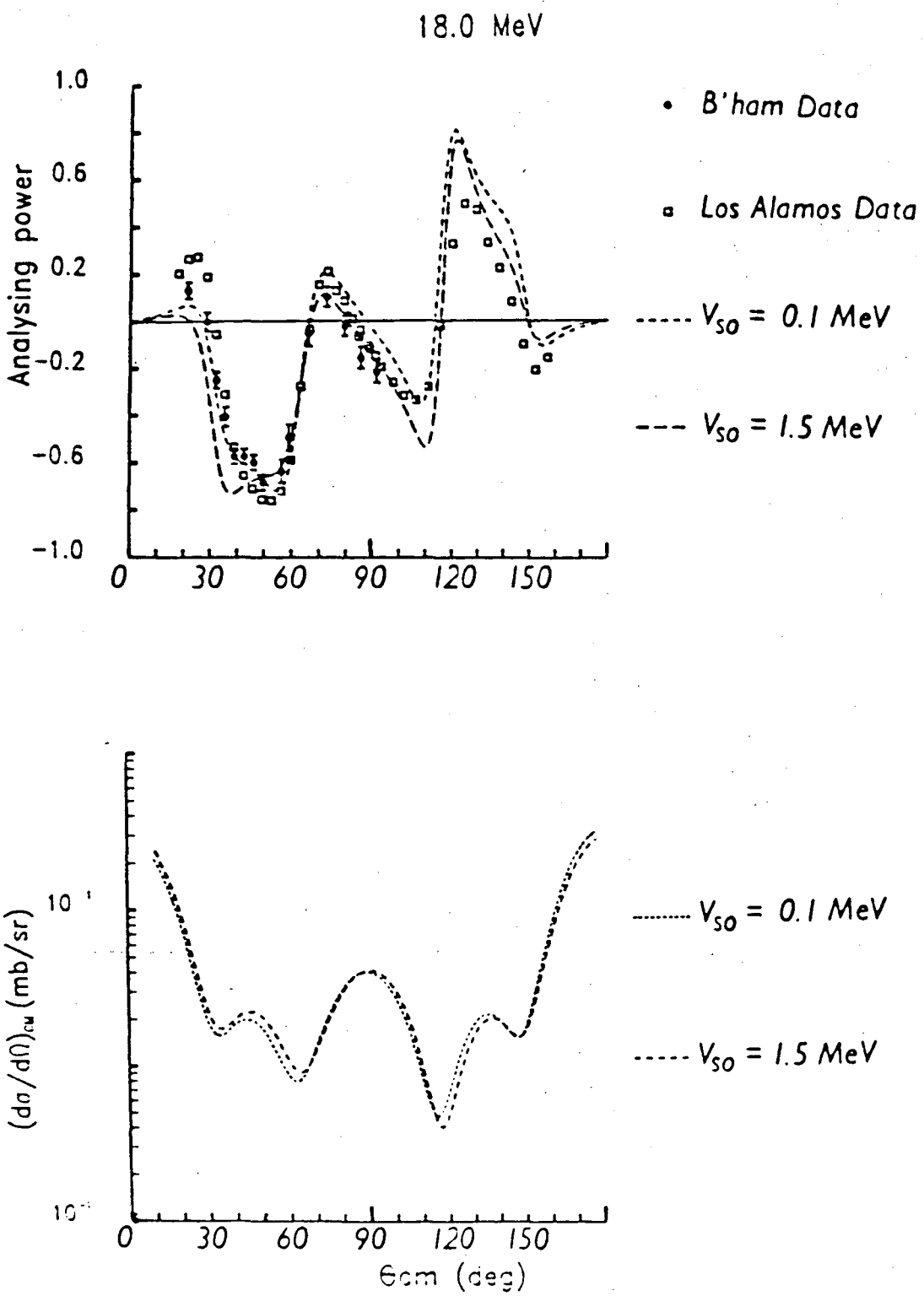

XBL 8711-5023

Fig. 10

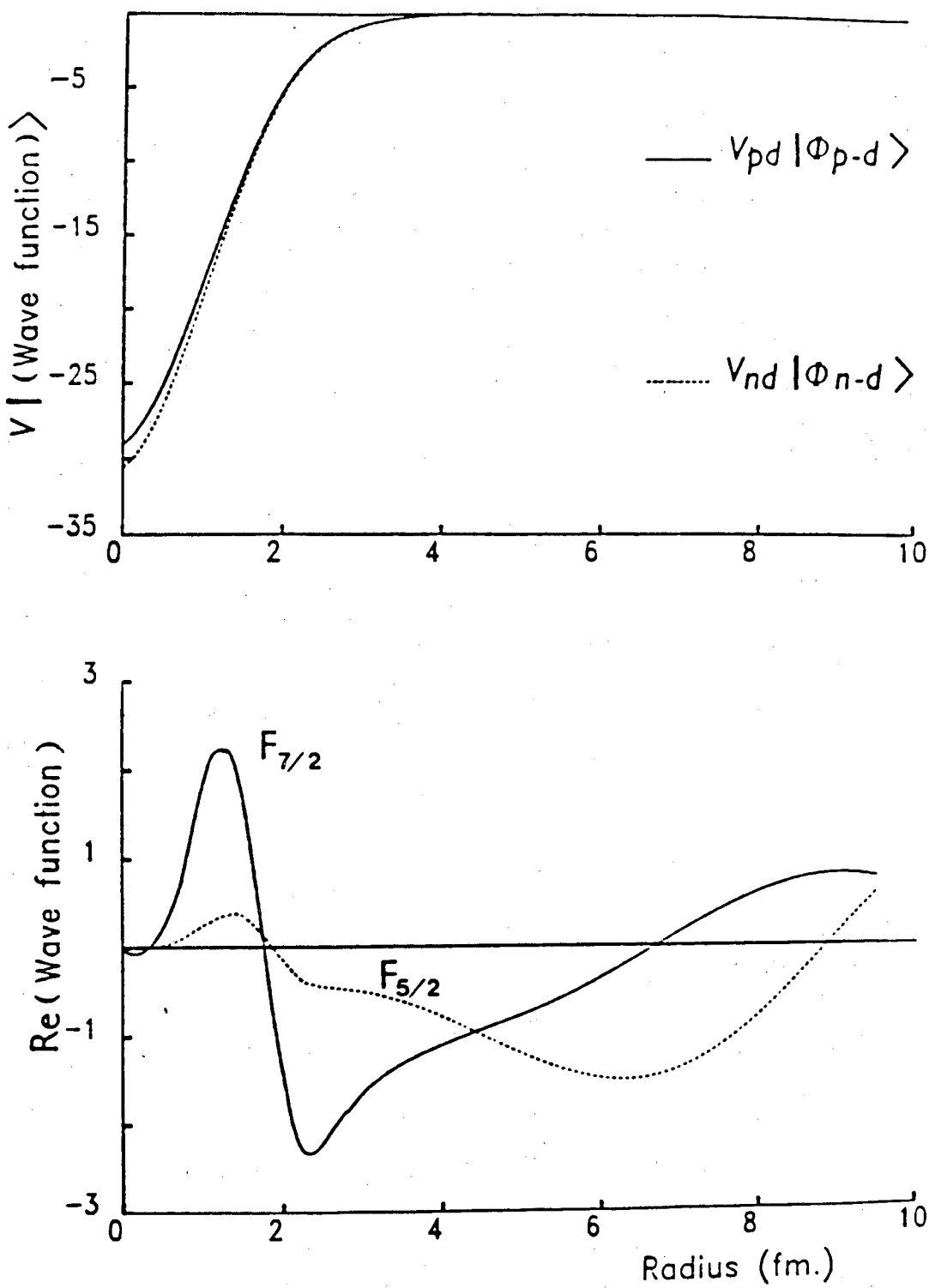

XBL 8711-5024

Fig. 11

LAWRENCE BERKELEY LABORATORY
TECHNICAL INFORMATION DEPARTMENT
UNIVERSITY OF CALIFORNIA
BERKELEY, CALIFORNIA 94720